

Finite concentration effects on diffusion-controlled reactions

Cite as: J. Chem. Phys. **121**, 7896 (2004); <https://doi.org/10.1063/1.1795132>

Submitted: 07 June 2004 . Accepted: 27 July 2004 . Published Online: 12 October 2004

Sanjib Senapati, Chung F. Wong, and J. Andrew McCammon



View Online



Export Citation

ARTICLES YOU MAY BE INTERESTED IN

[Concentration dependence of the rate of diffusion-controlled reactions](#)

The Journal of Chemical Physics **64**, 4551 (1976); <https://doi.org/10.1063/1.432087>

[Substrate concentration dependence of the diffusion-controlled steady-state rate constant](#)

The Journal of Chemical Physics **122**, 184902 (2005); <https://doi.org/10.1063/1.1887165>

[Kinetics of diffusion-influenced bimolecular reactions in solution. I. General formalism and relaxation kinetics of fast reversible reactions](#)

The Journal of Chemical Physics **86**, 1883 (1987); <https://doi.org/10.1063/1.452140>

Lock-in Amplifiers
up to 600 MHz



Finite concentration effects on diffusion-controlled reactions

Sanjib Senapati

Department of Chemistry and Biochemistry, University of California, San Diego, La Jolla, California 92093-0365

Chung F. Wong

Department of Chemistry and Biochemistry, University of Missouri, St. Louis, Missouri 63121

J. Andrew McCammon

Department of Chemistry and Biochemistry, University of California, San Diego, La Jolla, California 92093-0365; Howard Hughes Medical Institute, University of California, San Diego, La Jolla, California 92093-0365; and Department of Pharmacology, University of California, San Diego, La Jolla, California 92093-0365

(Received 7 June 2004; accepted 27 July 2004)

The algorithm by Northrup, Allison, and McCammon [*J. Chem. Phys.* **80**, 1517 (1984)] has been used for two decades for calculating the diffusion-influenced rate-constants of enzymatic reactions. Although many interesting results have been obtained, the algorithm is based on the assumption that substrate–substrate interactions can be neglected. This approximation may not be valid when the concentration of the ligand is high. In this work, we constructed a simulation model that can take substrate–substrate interactions into account. We first validated the model by carrying out simulations in ways that could be compared to analytical theories. We then carried out simulations to examine the possible effects of substrate–substrate interactions on diffusion-controlled reaction rates. For a substrate concentration of 0.1 mM, we found that the diffusion-controlled reaction rates were not sensitive to whether substrate–substrate interactions were included. On the other hand, we observed significant influence of substrate–substrate interactions on calculated reaction rates at a substrate concentration of 0.1M. Therefore, a simulation model that takes substrate–substrate interactions into account is essential for reliably predicting diffusion-controlled reaction rates at high substrate concentrations, and one such simulation model is presented here. © 2004 American Institute of Physics. [DOI: 10.1063/1.1795132]

I. INTRODUCTION

Reactions occurring in solutions of viscous fluids are often influenced by the diffusive encounter of the reactant molecules. Examples include reactions in enzyme catalysis, electron or proton transfer, fluorescence and phosphorescence quenching, growth of colloidal particles, etc.^{1,2} For these reactions, the diffusional approach of one reactant to the other is rate limiting when the subsequent transformation does not involve a large activation barrier. Various attempts have been made in the past to calculate the rates for these reactions.^{3–13} In most of these attempts, however, only the interactions between two reacting molecules (*A*,*B*) were taken into account. Interactions among *A* and among *B* were ignored. Here, we extend a previous simulation model¹⁴ to take interactions among *B* into account while considering a dilute solution of *A* such that no significant interactions among *A* occur.

Analytical expressions for diffusion-controlled rate constants can only be obtained for reactant molecules with simple shapes.^{11–13} For complicated molecules such as proteins with irregular shapes and anisotropic electrostatic potentials, or for systems in which a variety of interactions among the reactant molecules operate simultaneously, obtaining analytical solutions is not feasible. Thus, computer simulations have played an important role in simulating

more realistic systems.^{3–10} By implicitly modeling the effects of solvent on molecular interactions and dynamics, Brownian dynamics simulations have allowed long simulations to be carried out to study reactions occurring in complicated biological systems.

Northrup, Allison, and McCammon (NAM) (Refs. 3–6) proposed a method for calculating the rate constant of the diffusion-influenced reaction between two reactants *A* and *B*. While this method has been used in studying many enzymatic reactions for over two decades, it is based on the assumption that interactions among *A* and among *B* can be ignored. As a result of this assumption, one only needs to simulate the diffusion of one molecule of *A* towards one molecule of *B*. This assumption may no longer be valid when the concentration of one of the two species is high. In this work, we develop a simulation model that takes interactions among *B* into account, although we still ignore the direct interactions among *A*. This is a reasonable assumption for studying a solution in which the concentration of one of the species is sufficiently dilute. The simulation model is based on one developed earlier for studying the dynamical distribution of ions surrounding biomolecules.¹⁴ In this model, a biomolecule is surrounded by a finite number of ions determined by a specified ion concentration. All the interactions among the ions and between the ions and a biomolecule were taken into account. In using this model to

simulate the distribution of sodium and chloride ions surrounding polyalanine, it was found that the preferential binding of sodium ions was dependent upon the ion concentration in a rather complicated manner, suggesting that accurate calculations of reaction rate constants at high substrate concentrations may also require proper treatment of the interactions among the substrates surrounding the biomolecule.

Here, we describe an extension of the previous model¹⁴ for simulating the Brownian motion of ions surrounding a biomolecule, to allow calculation of the diffusion-controlled rate constant between an enzyme and small charged substrates, taking into account substrate interactions. We examine whether substrate interactions can significantly affect the diffusion-controlled reaction rate, and we provide quantitative models for calculating these rates. Two extreme cases were studied in this initial work. In one case, the ligand acted like an inhibitor so that an enzyme can no longer react with another ligand after it had reacted with a first one. In the other case, the enzyme had a very fast turnover rate so that every ligand reacted the moment it came into contact with the enzyme.

II. METHODS

The systems we study were composed of a protein at a low concentration and ligands at a finite concentration C . Although the simulation model can already deal with biomolecules with complex shape,¹⁴ the simulations here focused on simulating spherical proteins and substrates to facilitate comparison with analytical results when possible. The protein was modeled as a single sphere with radius 35 Å and molecular charge -8 (in an attempt to crudely model acetylcholinesterase¹⁵). The ligands were modeled as monovalent positively charged spheres with an exclusion radius of 3 Å, and a hydrodynamic radius of 4.5 Å (in an attempt to crudely model acetylcholine). In all simulations, the protein was held fixed at the center of the simulation box and a large number of substrates were allowed to diffuse around the protein with a diffusion coefficient D calculated from the hydrodynamic radius of the substrate. This is a reasonable approximation as the protein is significantly larger, and thus moves much slower, than the substrates.

The protein was considered to be isotropically reactive and reacted with a ligand upon collision. For the radii of the protein and ligand used in the simulation, this meant that a reaction occurred when the ligand-protein distance was $r_o = 38$ Å. As in our earlier work,¹⁴ periodic boundary conditions were applied to a basic simulation box. The simulation box was cubic but different dimensions were used in different simulations. We studied a series of systems which we divided into two categories. Systems 1–4 fell in the category of dilute solutions and systems 5–8 fell in the category of concentrated solutions. Systems 1–4 were composed of one protein and seven ligands in a box of volume $V = 500 \times 500 \times 500$ Å³. This corresponded to a ligand concentration of $C = 0.0001M$. Systems 5–8 were composed of one protein and 203 ligands in a box of volume $V = 150 \times 150 \times 150$ Å³. This corresponded to a ligand concentration of $C = 0.1M$. The systems in each category differed from each other by the interactions included in them. No ligand-protein

TABLE I. Defining the systems.

System	Concentration	Ligand-Ligand interactions	Ligand-Protein interactions
System 1	0.0001	No	No
System 2	0.0001	No	Yes
System 3	0.0001	Yes	No
System 4	0.0001	Yes	Yes
System 5	0.1	No	No
System 6	0.1	No	Yes
System 7	0.1	Yes	No
System 8	0.1	Yes	Yes

or ligand-ligand interaction were present in systems 1 and 5 so that the ligands diffused freely. In systems 2 and 6, the ligands did not interact with each other but interacted with the protein through a short-range hard-sphere potential (which was only used during the equilibration period to prevent the ligands from penetrating into the protein) plus a long-range Coulomb potential:

$$U_{L-P}(r) = u_{ip}^{HS}(r) + q_i q_p / \epsilon r, \quad (1)$$

where r was the distance between the i th ligand and the protein p , $u_{ip}^{HS}(r)$ was the hard sphere interaction potential which was equal to ∞ for $r < 38$ Å and zero elsewhere, q_i and q_p were the charges on ligand i and protein p , and ϵ was the dielectric coefficient. In systems 3 and 7, only ligand-ligand interactions were present. The ligands interacted among themselves through a Lennard-Jones plus Coulomb potential:

$$U_{L-L}(r) = \sum_i \sum_{j>i} 4 \epsilon_{ij} [(\sigma_{ij}/r)^{12} - (\sigma_{ij}/r)^6] + q_i q_j / \epsilon r. \quad (2)$$

Here, r was the distance between ligand i and ligand j , σ_{ij} and ϵ_{ij} were the usual Lennard-Jones parameters between ligands i and j , and q_i and q_j were the charges on ligands i and j . In systems 4 and 8 the protein interacted with the ligands through a short-range hard-sphere potential (which was only used during the equilibration period to prevent the ligands from penetrating into the protein) plus a long-range Coulomb potential. The ligands interacted among themselves through a Lennard-Jones plus Coulomb potential. The forms of the potentials were the same as those in Eqs. (1) and (2). Table I lists the interactions included in each of the eight systems. These systems were set up to facilitate comparisons with results from analytical theories, to evaluate deviations from the results for the NAM model, and to examine the significance of including ligand-ligand interactions on calculating reaction rates.

A dielectric constant of $\epsilon = 78$ was used throughout the system. The short-range interactions were truncated at 20 Å, and a 50 Å cutoff was used for the electrostatic interactions. In each simulation, the first 20 ns data were discarded. A production run was then carried out to produce snapshots for initiating reactive simulations. Snapshots separated by 10 ns were used. To obtain reasonable statistics for calculating the quantities described in Results and Discussions, at least 1000

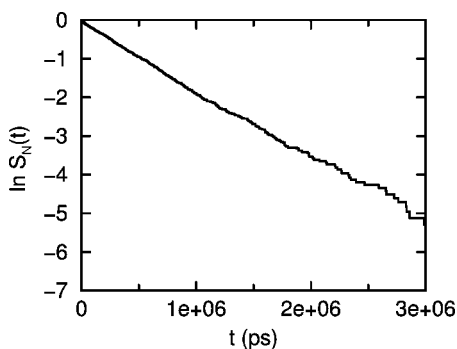


FIG. 1. The time dependence of $\ln S_N(t)$ for the system in which no molecular interactions were included (system 1). The ligand concentration was $0.0001M$.

of such configurations were used. While monitoring reaction starting from each of these snapshots, a time resolution of 1 ps was used.

The simulation model used the Ermak and McCammon algorithm¹⁶ to generate a trajectory of a system of N interacting/noninteracting particles. The equation of motion for following the Brownian motion of the particles takes the following form:

$$r_i(t + \delta t) = r_i(t) + D_i F_i \delta t / k_B T + R_i, \quad (3)$$

where $r_i(t)$ is the position of the i th ligand at time t , k_B is the Boltzmann constant, T is the absolute temperature which was taken to be 300 K, D_i is the diffusion constant of the ligand which was taken to be $0.545 \times 10^{-5} \text{ cm}^2/\text{s}$, F_i is the force exerted on particle i , δt is the time step, and R_i is the random displacement. A time step of 0.04 ps was used in this work.

III. RESULTS AND DISCUSSIONS

To follow the reaction rate, one can focus on the fate of the protein surrounded by N ligands. We use the survival probability of the protein to describe its fate after surrounding it with an equilibrium distribution of ligands at time $t = 0$. The survival probability $S_N(t)$ of the protein in the presence of N ligands at time t can be expressed as,⁸

$$\frac{dS_N(t)}{dt} = -Ck(t)S_N(t); \quad (4)$$

$$d \ln S_N(t) = -Ck(t)dt, \quad (5)$$

where C is the concentration of the ligand and $k(t)$ is the rate coefficient. Thus the slope of the linear plot of $\ln S_N(t)$ versus t can give us the rate coefficient. In Fig. 1 we present such a plot for system 1. System 1 was a dilute solution system with a ligand concentration $C = 0.0001M$. A linear least-squares fit through the data gave a rate constant $k_D^o = 1.8 \times 10^{10} M^{-1} \text{ s}^{-1}$. The main purpose of studying system 1 was to verify that our simulation model using the survival probability method could give reliable results for the reaction rate constant. System 1 represents one of the simplest model reactions for which an analytical solution is known. For a system with no interactions, the rate constant, k_D^o , is given by³

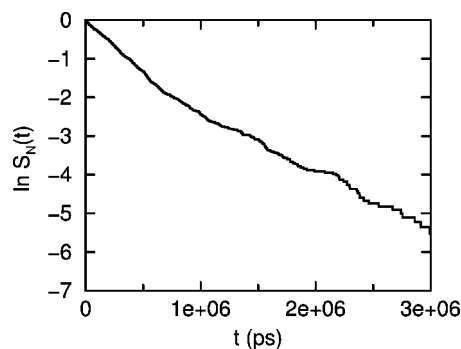


FIG. 2. The time dependence of $\ln S_N(t)$ for the system where the ligands interacted with the protein but did not interact with each other (system 2). The ligand concentration was $0.0001M$.

$$k_D^o = 4\pi D r_o, \quad (6)$$

where D is the relative diffusion constant between the two reacting particles and r_o is the separating distance below which reaction occurs. Using $r_o = 38 \text{ \AA}$ and $D = 0.545 \times 10^{-5} \text{ cm}^2/\text{s}$ one obtains $k_D^o = 1.6 \times 10^{10} M^{-1} \text{ s}^{-1}$. This matches our simulated result within the estimated error range ($1.8 \pm 0.3 \times 10^{10} M^{-1} \text{ s}^{-1}$).

If ligand–protein interactions exist for $r > r_o$ but are centrosymmetric in nature, the analytical solution for the rate constant is,³

$$k_D = \left(\int_b^\infty dr \left\{ \frac{\exp[U(r)/k_B T]}{4\pi r^2 D} \right\} \right)^{-1}, \quad (7)$$

where $U(r)$ is the potential of mean force between the protein and the ligand ($= q_l q_p / \epsilon r$ in the models studied here) and D is the relative diffusion coefficient, which equals the sum of the diffusion constants of the reacting particles when hydrodynamic interactions are ignored. Using $b = 38 \text{ \AA}$ and $D = D_L = 0.545 \times 10^{-5} \text{ cm}^2/\text{s}$ (the diffusion constant of the protein was much smaller and thus could be neglected), one obtains $k_D = 3.2 \times 10^{10} M^{-1} \text{ s}^{-1}$. This can be compared to the results from system 2, in which ligand–protein interactions were present but ligand–ligand interactions were not included. System 2 is a dilute solution with a ligand concentration of $0.0001M$. Figure 2 presents the time dependence of $\ln S_N(t)$ for this system. The computed rate constant obtained from a linear least-squares fit of the data was $k_D = 2.8 \times 10^{10} M^{-1} \text{ s}^{-1}$. Again, this is in reasonable agreement with the analytical result.

To test the validity of the NAM theory, which ignores ligand–ligand interactions, one can simply compare results obtained from a model in which no ligand interactions exist with those obtained from a model in which ligand interactions are present. We already had two systems, 1 and 2, in which no ligand–ligand interactions existed. Introducing ligand–ligand interactions converted system 1 into system 3 and system 2 into system 4. Comparing the $\ln S_N(t)$ versus t results between systems 1 and 3, and between systems 2 and 4 gives some insight into the significance of ligand–ligand interactions in influencing the reaction rates for this dilute solution with a $0.0001M$ ligand concentration. The results are shown in Fig. 3. The figure shows that ligand–ligand

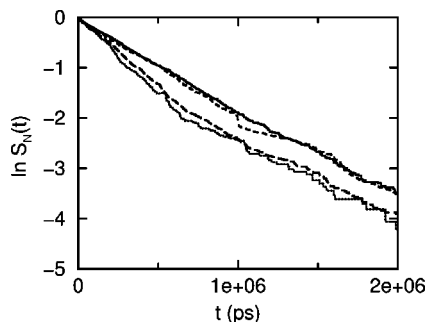


FIG. 3. A comparison of $\ln S_N(t)$ vs t for various systems with ligand concentration equal to $0.0001M$. The solid line is for the system in which the ligands did not interact with each other (system 1), the long dashed line is for the system in which only ligand–protein interactions were present (system 2), the dashed line is for the system in which only ligand–ligand interactions were included (system 3), and the dotted line is for the system in which both ligand–ligand and ligand–protein interactions were present (system 4).

interactions do not significantly influence the reaction rates for this dilute ligand concentration. Thus, as expected, the NAM theory works well at sufficiently low ligand concentrations.

We simulated four concentrated solutions at $0.1M$ by surrounding the protein with 203 ligands in a box with dimension 150 \AA^3 . In system 5, no ligand–protein or ligand–ligand interactions was present. A ligand–protein interaction potential was incorporated in system 6 to study the effects of protein–ligand electrostatic interactions on reaction rate. Systems 5 and 6 were then converted to system 7 and 8 by introducing ligand–ligand interactions. Figure 4 presents the variation of $\ln S_N(t)$ with time for all the four systems. As before, the electrostatic interactions between the protein and the ligands had a significant impact on reaction rate. More interesting, however, was the significant influence of ligand–ligand interactions on reaction rate at this higher ligand concentration. The plot for system 7 where ligand–ligand interactions were introduced now deviates from that of system 5. Similarly, the plot for system 8 deviates from that of system 6. In both cases, ligand–ligand interactions were seen to enhance the reaction rate.

In the above model, the enzyme was rendered inactive after reaction with a single ligand. We also constructed another model in which the enzyme was able to react with multiple ligands no matter how fast the next ligand came into contact with the enzyme after the previous one. As more

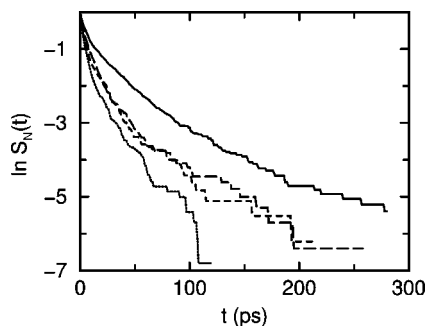


FIG. 4. Same as Fig. 3 except with a ligand concentration equal to $0.1M$.

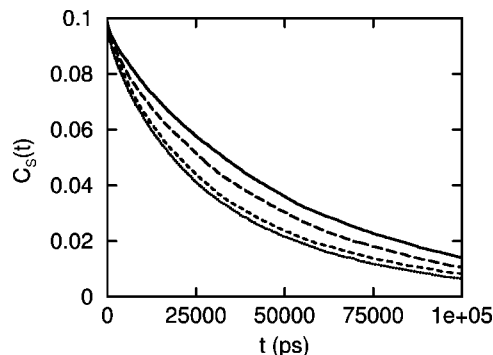


FIG. 5. A comparison of $C_s(t)$ vs t for systems with a ligand concentration equal to $0.1M$. The lines are the same as in Fig. 3.

ligands reacted, the concentration of the ligand gradually decreased. Figure 5 compares the time dependence of the variation of the ligand concentration, $C_s(t)$ for systems 5–8. A significant influence of the ligand–ligand interactions on the reaction rate is also evident from this model. Therefore, both simulation models for systems 5–8 concluded that there are significant deviations from the NAM results at high ligand concentrations, such as $0.1M$, for ligands that are singly charged and have a size similar to acetylcholine.

At higher ligand concentrations, it is hard to use these simulation models to obtain the steady-state rate constant at the long-time limit because most ligands react at earlier times. This is because many ligands are close to the enzyme in the equilibrium distribution before reactions are monitored when the ligand concentration is high. Accordingly, many trajectories need to be run to obtain good statistics for calculating the steady-state rate constant. Alternatively, one can calculate the potential of mean force (pmf) from the simulation and insert the pmf information into Eq. (7) to obtain a quantitative estimate of the rate constants.¹⁷ This step would be of interest when longer simulations can be done to obtain better sampling statistics.

IV. SUMMARY AND CONCLUSIONS

The Northrup–Allison–McCammon algorithm has been used extensively for calculating the diffusion-controlled reaction rates of enzymatic reactions. This algorithm neglects the interactions among the substrate molecules. We have constructed a simulation model that includes such interactions. The simulation model was first tested on simple systems for which analytical solutions are available. We then applied the model to study systems in which no rigorous analytical solution is feasible and examined the significance of substrate–substrate interactions on diffusion-controlled reaction rates. We found that the approximation of neglecting the substrate–substrate interactions is valid at low ligand concentrations, such as 0.1 mM , but that significant deviations from NAM occur at higher concentrations, such as $0.1M$. The ligand concentration can reach concentrations as high as $0.1M$ in real systems such as in synapses.¹⁸

ACKNOWLEDGMENTS

This work was supported in part by NIH, NSF, the Howard Hughes Medical Institute, the National Biological Computational Resource, the NSF Center for Theoretical Biological Physics, and the W. M. Keck Foundation.

¹S. A. Rice, *Comprehensive Chemical Kinetics 25, Diffusion-Limited Reactions* (Elsevier, Amsterdam, 1985).

²E. Kotomin and V. Kuzovkov, *Comprehensive Chemical Kinetics 34, Modern Aspects of Diffusion-Controlled Reactions* (Elsevier, Amsterdam, 1996).

³S. H. Northrup, S. A. Allison, and J. A. McCammon, *J. Chem. Phys.* **80**, 1517 (1984).

⁴S. A. Allison, S. H. Northrup, and J. A. McCammon, *J. Chem. Phys.* **83**, 2894 (1985).

⁵J. A. McCammon, S. H. Northrup, and S. A. Allison, *J. Phys. Chem.* **90**, 3901 (1986).

⁶S. H. Northrup, M. S. Curvin, S. A. Allison, and J. A. McCammon, *J. Chem. Phys.* **84**, 2196 (1986).

⁷S. Yang, J. Kim, and S. Lee, *J. Chem. Phys.* **111**, 10119 (1999).

⁸H. Zhou and A. Szabo, *J. Phys. Chem.* **100**, 2597 (1996).

⁹H. Zhou, *J. Phys. Chem.* **94**, 8794 (1990).

¹⁰G. Zou and R. D. Skeel, *Biophys. J.* **85**, 2147 (2003).

¹¹T. R. Waite, *Phys. Rev.* **107**, 463 (1957).

¹²D. F. Calef and J. M. Deutch, *Annu. Rev. Phys. Chem.* **34**, 493 (1983).

¹³K. Chou and G. Zhou, *J. Am. Chem. Soc.* **104**, 1409 (1982).

¹⁴W. Yu, C. F. Wong, and J. Zhang, *J. Phys. Chem.* **100**, 15280 (1996).

¹⁵S. Tara, A. H. Elcock, P. D. Kirchhoff, J. M. Briggs, Z. Radic, P. Taylor, and J. A. McCammon, *Biopolymers* **46**, 465 (1998).

¹⁶D. L. Ermak and J. A. McCammon, *J. Chem. Phys.* **69**, 1352 (1978).

¹⁷H. Zhou and A. Szabo, *J. Chem. Phys.* **95**, 5948 (1991).

¹⁸K. Tai, S. D. Bond, H. R. MacMillan, N. A. Baker, M. J. Holst, and J. A. McCammon, *Biophys. J.* **84**, 2234 (2003).